# Brightness and color of rapidly moving objects: The visual appearance of a large sphere revisited

U. Kraus
*Theoretische Astrophysik, Universität Tübingen, Auf der Morgenstelle 10C, 72076 Tübingen, Germany*

(Received 31 March 1998; accepted 9 March 1999)

An object at relativistic speed is seen as both rotated and distorted when it is large or close by so that it subtends a large solid angle. This is a consequence of the aberration effect and is obtained by purely geometric considerations. In this paper it is pointed out and illustrated that a photorealistic image of such an object would actually be dominated by the Doppler and searchlight effects, which would be so prominent as to render the geometric apparent shape effectively invisible. © *2000 American Association of Physics Teachers.*

## I. INTRODUCTION

Interest in the visual appearance of objects moving with velocities close to the speed of light was triggered by the question of the visibility of the Lorentz contraction. The first discussion, given by Lampa as early as 1924,[1] remained largely unnoticed, but the question was rediscovered in 1959. It was subsequently shown that the apparent length of a meter stick in a visual or photographic observation is not the Lorentz-contracted length[1–4] and that quite generally, objects subtending a small solid angle appear rotated but otherwise undistorted,[2,5] whereas objects subtending a large solid angle are seen as both rotated and distorted. A particularly intriguing result of these considerations is the fact that a sphere always presents a circular outline whatever its speed and its angular size may be.[4,6–9] All of these results are based on the aberration effect and are purely geometrical in nature.

Brightness and color are likewise important aspects of the visual appearance of rapidly moving objects. They are determined by the Doppler effect and the transformation of light power (searchlight effect) and have been studied in connection with the appearance of the celestial sphere from a relativistic spaceship.[10,11] While objects subtending a small solid angle appear uniformly brighter (or dimmer) when moving toward (or away from) the observer, objects subtending a large solid angle suffer nonuniform Doppler and searchlight effects. In this paper it is pointed out that in the case of large objects, the Doppler and searchlight effects may dominate the visual impression of the object and create an image that is quite different from what the purely geometrical computation may lead one to expect.

In particular, when visualization tools are used to obtain images that give the impression of being virtually photorealistic images,[12,13] it is indispensable to allow for Doppler effect, searchlight effect, and also for the response of the human eye in order to obtain images that are realistic in the sense of being physically correct.

The computation of color and brightness of rapidly moving objects provides, on the one hand, an interesting and unusual application of colorimetry and, on the other hand, a practical illustration of the predictions of the special theory of relativity.

## II. BRIGHTNESS PERCEIVED BY THE HUMAN EYE

In order to compute the brightness of a rapidly moving object, consider a point on the surface of the object and a light ray that is emitted by this point and is received in the observer's eye (Fig. 1). The light ray makes some angle $\theta$ with the velocity $\mathbf{v}$ of the object.

The light ray can be completely specified in terms of the specific intensity or surface brightness, i.e., the amount of radiant energy per time per wavelength interval per solid angle and per area perpendicular to the direction of the ray, $I'(\lambda')$, in the rest frame of the object.

In the observer's rest frame, the radiation is observed with the Doppler-shifted wavelength

$$\lambda = \gamma(1-\beta\cos\theta)\lambda' =: \lambda'/d \tag{1}$$

[with the usual designations $\gamma=(1-\beta^2)^{-1/2}$, $\beta=v/c$, $c$ the speed of light], and with specific intensity

$$I(\lambda) = d^5 I'(\lambda' = \lambda d). \tag{2}$$

A derivation of Eq. (2) is given in the Appendix.

As an application, consider a view of the sun from a relativistic spaceship. The emission in the rest frame of the sun is approximately a blackbody spectrum,

$$I'(\lambda') = \frac{2hc^2}{\lambda'^5}\frac{1}{(e^{hc/k_B T'\lambda'}-1)} \tag{3}$$

(where $h$ is the Planck constant and $k_B$ the Boltzmann constant) with temperature $T'=5780\,\mathrm{K}$. Under the transformation (2) this turns into an observed spectrum which is again a blackbody spectrum but with temperature $T=T'd$. Figure 2 shows the rest frame spectrum and observed spectra for $d=0.8$ and $d=1.2$.

The apparent brightness of the surface of the moving object is the result of the perception of the observed spectrum $I(\lambda)$ by the human eye. The perceived brightness is therefore determined solely by the visible part of the spectrum ($400\,\mathrm{nm}<\lambda<800\,\mathrm{nm}$) and depends on the response of the human eye to light stimuli of different wavelengths.

Human visual perception is quantified using colorimetry. Colorimetric applications are based on the ''1931 CIE Standard Observer'' defined by the ''Commission Internationale de l'Eclairage'' (or CIE) on the basis of experimental data. Using the CIE-color-matching function $y(\lambda)$ whose values are tabulated at 1-nanometer intervals[14] (see also Fig. 2), the perceived brightness associated with the observed spectrum $I(\lambda)$ is

$$Y = \int I(\lambda)y(\lambda)d\lambda. \tag{4}$$

Applied to the spectra in Fig. 2 one obtains $Y(d=0.8)$

  

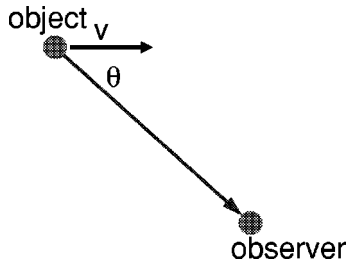


Fig. 1. A light ray from the moving object to the observer.

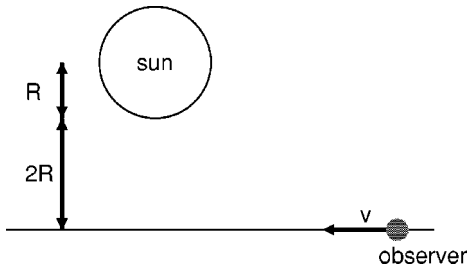


Fig. 3. Path of relativistic spaceship passing the sun at a distance of three solar radii from its center.

$=88$, $Y(d=1.0)=273$ and $Y(d=1.2)=548$ in arbitrary units of brightness.

When a rapidly moving object is large or close by so that it subtends a large solid angle, then different values of $d$ will be computed for different points on the surface. This will, in general, produce substantially different levels of apparent brightness.

As an example consider the view of the sun from a relativistic spaceship on the path indicated in Fig. 3. When the spaceship approaches the sun, the Doppler factor $d$ is large and therefore the perceived brightness $Y$ is also large. While the spaceship passes the sun and finally leaves it behind, the apparent brightness decreases continually until the sun appears much fainter than for an observer in the solar rest frame.

While the spaceship is close by, the sun subtends a large solid angle. Images of the sun as seen at different spaceship velocities have been computed with the procedure sketched in Fig. 4: Each surface element of a fictitious image plane is assigned the surface brightness of the object surface that is seen through it.[15] The sun being a sphere, its geometric apparent shape always has a circular outline. The size of the image[4] is largest when the sun is seen at $\theta=\pi/2$, i.e., perpendicular to the direction of motion, and this largest image has the same size for every velocity. In fact, the maximum half-angle $\alpha_{\max}$ is given by $\sin\alpha_{\max}=R/D$, where $R$ is the radius of the sphere and $D$ the distance of closest approach to the center of the sphere. For a spaceship on the path shown in Fig. 3, $\alpha_{\max}=19.5°$. (To prevent distortion in wide angle images like these the image should ideally fill the same field of view when viewed as when created.)

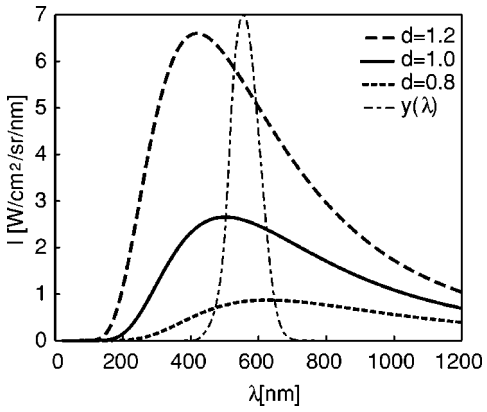


Fig. 2. Blackbody spectrum with temperature $T=5780$ K in its rest frame ($d=1$) and observed spectra for $d=0.8$ and $d=1.2$. The color-matching function $y(\lambda)$ (dash-dotted line) is the weighting function for the computation of the perceived brightness.

Images of the sun as seen at different spaceship velocities at $\theta=\pi/2$ are shown in Fig. 5. At low velocities the circular outline of the image is clearly visible. However, at high velocities one side of the sun appears to be so bright that it outshines the rest of the spherical disk and the sun is actually seen in the shape of a crescent.

## III. CONCLUDING REMARKS

The perceived color of a rapidly moving object can be computed in much the same way as the brightness. With the CIE-color-matching functions $x(\lambda)$ and $z(\lambda)$ one finds $X=\int I(\lambda)x(\lambda)d\lambda$ and $Z=\int I(\lambda)z(\lambda)d\lambda$. These two quantities have no simple intuitive physical meaning, but the triplet $(X,Y,Z)$ is a unique description of the perceived color which can be transformed into any other color representation, e.g., the RGB color space of a monitor.

When a moving object subtends a large solid angle, so that different values of $d$ are computed for different points on the surface, then in principle a unicolored object should appear to be multicolored. However, different colors are associated with different levels of brightness and brightness changes tend to be much more drastic than color changes. In a color version of Fig. 5, e.g., the upper five images of the sun appear white or nearly white, while the bright parts of the lower two images appear ochre and red, respectively. In the sixth image, the right-hand side of the disk should appear orange, but is so faint that the color is not visible and the visual impression is that of a unicolored ochre crescent.

It is the visible part of the transformed spectrum $I(\lambda)$ that determines both the perceived brightness and color. This is radiation that has been Doppler shifted into the visible range; it may belong to the ultraviolet or infrared or even the radio range of the rest frame spectrum. For $\beta=0.9$, for example, the Doppler factor $d$ varies between $d=0.23$ for $\theta=0$ and $d=4.36$ for $\theta=\pi$. In order that the visible parts of the transformed spectra for all possible values of $d$ can be computed, the rest frame spectrum must be specified between $\lambda'=90$ nm (far ultraviolet) and $\lambda'=3500$ nm (infrared).

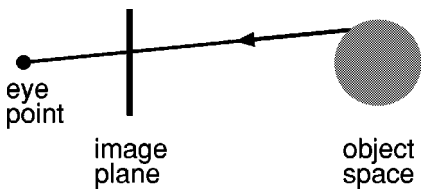


Fig. 4. Image generation: Each surface element of a fictitious image plane is assigned the surface brightness of the object that is seen through it.

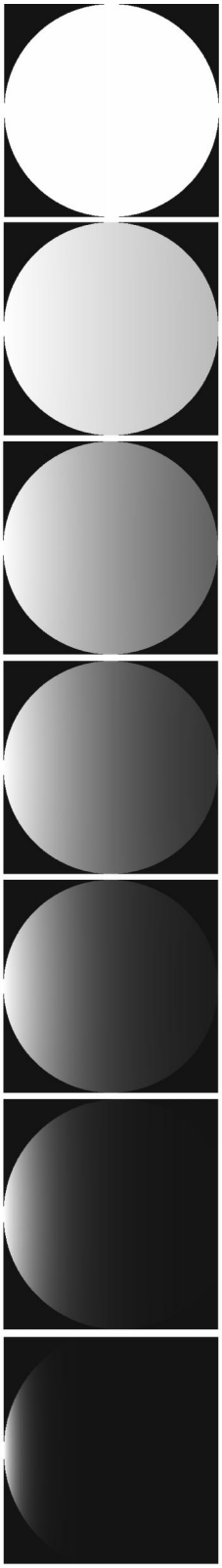

Fig. 5. The sun seen from a relativistic spaceship at relative velocities $v/c=0$, 0.1, 0.3, 0.5, 0.7, 0.9, and 0.99 (top to bottom). The spaceship follows the path shown in Fig. 3 and the sun is observed in the direction $\theta=\pi/2$. Since the brightness levels differ substantially, the pixel values in the different images are not to scale. The brightest pixel corresponds to $Y=273$, 310, 352, 323, 195, 18, and $2.6\times10^{-5}$, respectively (top to bottom), in arbitrary units of brightness. Lines of constant $\theta$ are faintly visible because brightness is displayed in 256 discrete levels.

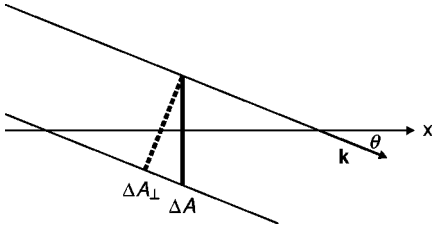


Fig. 6. Beam of photons in direction **k**, surface element $\Delta A$, and its projection $\Delta A_\perp$.

It has been demonstrated how standard graphics tools can be applied to scenes involving objects and light sources at relativistic speeds.[12,13] This may well be the most promising approach to the visualization of relativistic effects, especially for realistic images of complex scenes. However, the images obtained so far are not realistic in the sense of being physically correct: The transformation of the specific intensity has either been neglected or has been applied incorrectly.

## ACKNOWLEDGMENTS

My thanks to Hanns Ruder, Daniel Weiskopf, and Corvin Zahn for valuable discussions.

## APPENDIX: LORENTZ TRANSFORMATION OF THE SPECIFIC INTENSITY

Transformations of light power from an unresolved source have been given by McKinley and Doherty[11] and McKinley.[16,17] Burke and Strode[18] derive the transformation of the intensity of a resolved object for the special case of observation at right angles to the direction of motion; the general case is treated by Peebles[19] and by Greber and Blatter.[20]

The following derivation of the Lorentz transformation of the specific intensity gives the transformation law for spectrally resolved light power emitted by a resolved object. Like most of the derivations mentioned above it is based on a photon-counting argument.

The transformation is done between two standard frames of reference $S$ and $S'$, $S'$ moving with velocity $v$ in the $x$ direction with respect to $S$. The quantity to be transformed is the specific intensity, i.e., the radiant energy per unit time per unit solid angle per unit interval of photon energy and per unit area perpendicular to the beam. This quantity is related to photon numbers in the following way.

Consider a beam of photons with photon energy between $E$ and $E+\Delta E$, incident in the solid angle $\Delta\Omega$ around the direction **k** and choose a surface $\Delta A$. Count the photons in the beam that pass the surface during time $\Delta t$. From the number $N$ of counted photons, compute the specific intensity $I(\mathbf{k},E)$ which is by definition given by

$$NE=I\Delta E\Delta\Omega\Delta A_\perp\Delta t, \tag{5}$$

where $\Delta A_\perp$ is the projection of $\Delta A$ onto a plane perpendicular to **k**. In particular, if the normal of $\Delta A$ points in the $x$ direction, then

$$\Delta A_\perp=\Delta A\cos\theta, \tag{6}$$

with the angle $\theta$ between the photon beam direction **k** and the $x$ axis (Fig. 6).

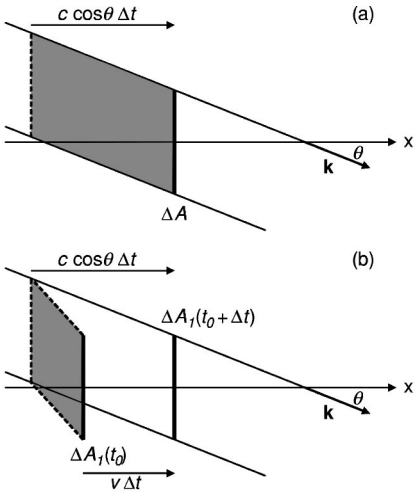


Fig. 7. (a) Photons contained in the shaded volume at time $t_0$ will pass the surface $\Delta A$ between $t_0$ and $t_0+\Delta t$. (b) Photons contained in the shaded volume at time $t_0$ will pass the moving surface $\Delta A_1$ between $t_0$ and $t_0+\Delta t$.

The velocity of the photons in the beam has the $x$ component $c\cos\theta$. The $N$ photons that pass $\Delta A$ between $t_0$ and $t_0+\Delta t$ are therefore just those photons that are contained in the shaded volume in Fig. 7(a) at time $t_0$. This volume has the size

$$\Delta V=\Delta A c\cos\theta\Delta t. \tag{7}$$

As a preliminary to the Lorentz transformation of the intensity, repeat the counting experiment for a surface $\Delta A_1$ with the same size and orientation as $\Delta A$ and moving with velocity $v$ in the $x$ direction.

All photons that are contained in the shaded volume in Fig. 7(b) at time $t_0$ will pass $\Delta A_1$ between $t_0$ and $t_0+\Delta t_0$. This volume has the size

$$\Delta V_1=\Delta A_1(c\cos\theta-v)\Delta t \tag{8}$$

and is smaller than $\Delta V$ by a factor $(\cos\theta-\beta)/\cos\theta$. The number of photons that pass $\Delta A_1$ during $\Delta t$ is smaller than $N$ by the same factor:

$$N_1E=I\Delta E\Delta\Omega\Delta A_1\cos\theta\Delta t(\cos\theta-\beta)/\cos\theta. \tag{9}$$

In order to relate the values of the intensity in $S$ and $S'$, describe the counting of the same $N_1$ photons from the point of view of an observer in $S'$ where the surface $\Delta A_1$ is at rest.

In $S'$ the photons in the beam have the Doppler-shifted energy

$$E'=E\gamma(1-\beta\cos\theta)=:E/d \tag{10}$$

and, because of aberration, make an angle $\theta'$ with the $x'$ axis where

$$\cos\theta'=\frac{\cos\theta-\beta}{1-\beta\cos\theta}. \tag{11}$$

The counting is sustained over a time

$$\Delta t'=\Delta t/\gamma \tag{12}$$

and since the surface area $\Delta A_1$ is perpendicular to the relative motion of $S$ and $S'$,

$$\Delta A_1'=\Delta A_1. \tag{13}$$

The specific intensity $I'(\mathbf{k}',E')$ is related to $N_1$ by

$$N_1E'=I'\Delta E'\Delta\Omega'\Delta A_1'\cos\theta'\Delta t'. \tag{14}$$

Dividing Eq. (9) by Eq. (14) it is found that

$$\frac{I}{I'}=\frac{E}{E'}\frac{\Delta E'}{\Delta E}\frac{\Delta\Omega'}{\Delta\Omega}\frac{\Delta A_1'}{\Delta A_1}\frac{\Delta t'}{\Delta t}\frac{\cos\theta'}{\cos\theta-\beta}. \tag{15}$$

Relation (11) between $\theta'$ and $\theta$ gives the transformation of elements of solid angle:

$$\frac{d\Omega'}{d\Omega}=\frac{\sin\theta'}{\sin\theta}\frac{d\theta'}{d\theta}=\frac{d\cos\theta'}{d\cos\theta}=\frac{1}{\gamma^2(1-\beta\cos\theta)^2}=d^2. \tag{16}$$

Inserting Eqs. (10)–(13) and (16) into (15) one obtains

$$\frac{I}{I'}=d\frac{1}{d}d^2 1\frac{1}{\gamma}\frac{1}{(1-\beta\cos\theta)}=d^3$$

or

$$\frac{I}{E^3}=\frac{I'}{E'^3}. \tag{17}$$

Often the specific intensity is expressed in terms of wavelength rather than photon energy. With $\lambda=hc/E$, photon energies in $\Delta E$ correspond to wavelengths in $\Delta\lambda=(hc/E^2)\Delta E$. From $I(\lambda)\Delta\lambda=I(E)\Delta E$ one finds

$$I(\lambda)=I(E)(E^2/hc) \tag{18}$$

and

$$\frac{I(\lambda)}{I'(\lambda')}=\frac{I(E)}{I'(E')}\frac{E^2}{E'^2}=d^5, \tag{19}$$

i.e., Eq. (2).

The transformation law of the integrated intensity is easily obtained from (17) or (19):

$$\int I(\lambda)d\lambda=d^4\int I'(\lambda')d\lambda'. \tag{20}$$


[1] A. Lampa, ''Wie erscheint nach der Relativitätstheorie ein bewegter Stab einem ruhenden Beobachter?'' Z. Phys. **72**, 138–148 (1924).
[2] J. Terrell, ''Invisibility of the Lorentz Contraction,'' Phys. Rev. **116**, 1041–1045 (1959).
[3] R. Weinstein, ''Observation of Length by a Single Observer,'' Am. J. Phys. **28**, 607–610 (1960).
[4] M. L. Boas, ''Apparent Shape of Large Objects at Relativistic Speeds,'' Am. J. Phys. **29**, 283–286 (1961).
[5] V. F. Weisskopf, ''The visual appearance of rapidly moving objects,'' Phys. Today **13** (9), 24–27 (1960).
[6] R. Penrose, ''The Apparent Shape of a Relativistically Moving Sphere,'' Proc. Cambridge Philos. Soc. **55**, 137–139 (1959).
[7] G. D. Scott and H. J. van Driel, ''Geometrical Appearances at Relativistic Speeds,'' Am. J. Phys. **38**, 971–977 (1970).
[8] D. Hollenbach, ''Appearance of a rapidly moving sphere: A problem for undergraduates,'' Am. J. Phys. **44** (1), 91–93 (1975).
[9] K. G. Suffern, ''The apparent shape of a rapidly moving sphere,'' Am. J. Phys. **56**, 729–733 (1988).
[10] S. Moskowitz, ''Visual Aspects of Trans-Stellar Space Flight,'' Sky Telesc. **33**, 290–294 (1967).
[11] J. M. McKinley and P. Doherty, ''In search of the 'starbow:' The appearance of the starfield from a relativistic spaceship,'' Am. J. Phys. **47**, 309–316 (1979).
[12] P.-K. Hsiung, R. H. Thibadeau, C. B. Cox, R. H. P. Dunn, M. Wu, and P. A. Olbrich, ''Wide-band Relativistic Doppler Effect Visualization,'' Proceedings of the Visualization '90 Conference, 1990 (unpublished).

[13]M.-C. Chang, F. Lai, and W.-C. Chen, ''Image Shading Taking into Account Relativistic Effects,'' ACM Trans. Graphics **15** (4), 265–300 (1996).
[14]G. Wyszecki and W. S. Stiles, *Color Science* (Wiley, New York, 1982), pp. 240–252.
[15]R. Hall, *Illumination and Color in Computer Generated Imagery* (Springer-Verlag, New York, 1989), pp. 2–5.
[16]J. M. McKinley, ''Relativistic transformations of light power,'' Am. J. Phys. **47**, 602–605 (1979).
[17]J. M. McKinley, ''Relativistic transformation of solid angle,'' Am. J. Phys. **48**, 612–614 (1980).
[18]J. R. Burke and F. J. Strode, ''Classroom exercises with the Terrell effect,'' Am. J. Phys. **59**, 912–915 (1991).
[19]P. J. E. Peebles, *Principles of Physical Cosmology* (Princeton U.P., Princeton, NJ, 1993), pp. 154–157.
[20]T. Greber and H. Blatter, ''Aberration and Doppler shift: The cosmic background radiation and its rest frame,'' Am. J. Phys. **58** (10), 942–945 (1990).

## THE STIFLING GRIP OF RELIGION

I consider that the survival of religion and the antireductionism that it represents survives merely because it is so deeply ingrained in our cultural attitudes, and its survival is independent of its intrinsic truth. The stifling grip of religion on Man's mind stems partly from its early start, when, as our ancestors dropped from the trees they first sought explanations and solace; it also stems partly from religion's control (for both benevolent and malevolent purposes) of the behaviour of individuals and societies, and it stems partly from its capture of the literature and the arts, which has given it a powerful imagery. Someone with a fresh mind, one not conditioned by upbringing and environment, would doubtless look at science and the powerful reductionism that it inspires as overwhelmingly the better mode of understanding the world, and would doubtless scorn religion as sentimental wishful thinking. Would not that same uncluttered mind also see the attempts to reconcile science and religion by disparaging the reduction of the complex to the simple as attempts guided by muddle-headed sentiment and intellectually dishonest emotion?

P. W. Atkins, ''The Limitless Power of Science,'' in *Nature's Imagination—The Frontiers of Scientific Vision*, edited by John Cornwell (Oxford University Press, New York, 1995).